

How to Sum Contributions into the Total Charged-Current Neutrino–Nucleon Cross Section

Konstantin S. Kuzmin,^{1,3,*} Vladimir V. Lyubushkin,^{2,4,†} and Vadim A. Naumov^{1,5,‡}

¹*Bogoliubov Laboratory of Theoretical Physics, Joint Institute for Nuclear Research, RU-141980 Dubna, Russia*

²*Dzhelepov Laboratory of Nuclear Problems, Joint Institute for Nuclear Research, RU-141980 Dubna, Russia*

³*Institute for Theoretical and Experimental Physics, RU-117259 Moscow, Russia*

⁴*Physics Department of Irkutsk State University, RU-664003 Irkutsk, Russia*

⁵*INFN, Sezione di Firenze, I-50019 Sesto Fiorentino (FI), Italy*

(Dated: June 14, 2021)

The total CC (anti)neutrino-nucleon cross section is usually estimated by the sum of contributions from quasi-elastic scattering (QES), single-pion production through baryon resonances (RES), and deep inelastic scattering (DIS) with an appropriate scratching the phase space of the RES and DIS contributions. However the resulting total cross section is very sensitive to the value of the cut-off in invariant mass of the final hadron system produced in RES and DIS. We examine available experimental data on the QES and total CC cross sections in order to extract the best-fit value for this cut-off. By using the same data set we attempt to adjust the poorly known values of the axial mass for QES and RES.

PACS numbers: 12.15.Ji, 13.15.+g, 14.20.Gk, 23.40.Bw, 25.30.Pt

I. INTRODUCTION

It is conventional to estimate the inclusive charged and neutral current neutrino–nucleon cross sections by the sum of contributions from exclusive channels and deep inelastic scattering (DIS):

$$\sigma_{\nu N}^{\text{tot}} = \sigma_{\nu N}^{(\text{Q})\text{ES}} \oplus \sigma_{\nu N}^{1\pi} \oplus \sigma_{\nu N}^{2\pi} \oplus \dots \oplus \sigma_{\nu N}^{1K} \oplus \dots \oplus \sigma_{\nu N}^{\text{DIS}}. \quad (1)$$

In the absence of a received model for multi-hadron exclusive neutrino production, the exclusive contributions in Eq. (1) are usually assumed to be saturated by elastic (NC case) or quasielastic (CC case) scattering (ES/QES) and single-pion production through baryon resonances (RES). The exclusive and inclusive (DIS) contributions are of the same order of magnitude within the few-GeV energy region. Thus, to avoid double counting, the phase space of the RES and DIS contributions have to be scratched by the conditions $W < W_{\text{cut}}^{\text{RES}}$ and $W > W_{\text{cut}}^{\text{DIS}}$, respectively, where W is the invariant mass of the final hadron system in RES or DIS, and $W_{\text{cut}}^{\text{RES}}$ and $W_{\text{cut}}^{\text{DIS}}$ are some parameters.

The physical basis of this approximation is the concept of quark-hadron duality, according to which the resulting total cross section should be essentially independent of the specific values of the cutoff parameters if they are of the order of the threshold value of W for two-pion production, $W_{2\pi} = M_N + 2m_\pi \approx 1.2$ GeV. In practice, this value is too small since the structure functions involved into the calculations of the DIS cross section cannot be

extrapolated to the two-pion production threshold due to the obvious reasons.

The problem is aggravated by the uncertainties in the knowledge of the simplest exclusive contributions: the description of the RES reactions is vastly model-dependent and, even within a fixed model for RES, both RES and (Q)ES cross sections are very sensitive to the poorly known shape of the weak axial-vector form factors. By adopting the standard dipole parametrization for these form factors, their shapes can be described with the two phenomenological parameters (“axial masses”) M_A^{QES} and M_A^{RES} which, strictly speaking, may be different and whose experimental values spread within inadmissibly wide ranges [1].

In this study we attempt to fine-tune both the axial masses M_A^{QES} , M_A^{RES} and the cutoffs $W_{\text{cut}}^{\text{RES}}$, $W_{\text{cut}}^{\text{DIS}}$ by fitting available experimental data on the QES with $\Delta Y = 0$ and total CC cross sections for ν_μ and $\bar{\nu}_\mu$ scattering off different nuclear targets (converted to the proton, neutron, and isoscalar nucleon) as well as the independently measured ratios of these cross sections. For the moment, our global likelihood analysis does not include the experimental data for the (quasi)elastic reactions with $\Delta Y \neq 0$, the reactions of single-meson production and NC induced (exclusive and inclusive) reactions. However, the bulk of the data involved into the analysis is already rather representative and (more important) more self-consistent in comparison with the data for the single- and multi-hadron neutrino production and the NC reactions of any kind. Hence we guess it is sufficient for preliminary practical conclusions.

*Electronic address: kkuzmin@theor.jinr.ru

†Electronic address: lvv@nusun.jinr.ru

‡Electronic address: vnaumov@theor.jinr.ru;

URL: <http://theor.jinr.ru/~vnaumov/>

II. THEORETICAL MODELS

A. Quasielastic scattering

For the $\nu n \rightarrow \mu^- p$ and $\bar{\nu} p \rightarrow \mu^+ n$ cross sections we use the standard result (see, e.g., Ref. [2]) neglecting the second-class current contributions. For the elastic electromagnetic form factors $G_E^{p,n}$ and $G_M^{p,n}$ we apply the QCD Vector Meson model by Gari and Krümpelmann [3] extended and fine-tuned by Lomon [4] to match the current and consistent earlier experimental data derived using Rosenbluth separation and polarization transfer techniques. More explicitly, we explore the so-called ‘‘GKex(02S)’’ version of the model advocated by Lomon. At 4-momentum transfer Q^2 below $10 - 15 \text{ GeV}^2$, the GKex(02S) model is very close numerically to the PTD (polarization transfer data based) version of the popular ‘‘BBA-2003’’ inverse-polynomial parametrization by Budd *et al.* [5] obtained through a global fit to the world data on the Sachs form factors, including the results of several more recent measurements. Although the up-to-date experiments (see, e.g., numerous reports in Ref. [6]) do not contradict to both models, we prefer the GKex(02S) model since it meets the requirements of dispersion relations and QCD asymptotics at low and high Q^2 , while the BBA-2003 PTD fit has an unphysical behaviour when extrapolated to high Q^2 (a typical drawback of polynomial approximations).

For the axial and pseudoscalar form factors we use the conventional representations [2]

$$F_A(Q^2) = F_A(0) \left(1 + \frac{Q^2}{M_A^2}\right)^{-2}$$

and

$$F_P(Q^2) = \frac{2M_N^2}{m_\pi^2 + Q^2} F_A(Q^2),$$

with $F_A(0) = g_A = -1.2695$ [7]. The currently available experimental data on the axial mass, $M_A = M_A^{\text{QES}}$, show very wide spread, from roughly 0.6 to $1.2 \text{ GeV}/c^2$ [1]. Today, it is the main source of uncertainties in the QES cross sections. Since the pseudoscalar contribution enters into the cross sections multiplied by $(m_{e,\mu,\tau}/M_N)^2$, it is substantial for neutrino production of τ leptons but small for electron and muon production; hence the related uncertainty is not important for the present study.

Since the major part of the experimental data on QES obtained for heavy nuclear targets was not corrected for nuclear effects, one has to take these into account in calculations. We apply the simple Pauli factor since its effect for the total cross sections is not essentially different from that evaluated with the more sophisticated approaches.

B. Resonance single-pion production

In order to describe the single-pion neutrino production through baryon resonances we use an extended version of the model by Rein and Sehgal (RS) [8, 9]. The RS model, being one of the most circumstantial and approved phenomenological approaches to calculating the RES cross sections, is now incorporated into essentially all Monte Carlo neutrino event generators developed for both accelerator and astroparticle experiments. Our extension [10, 11] takes into account the final lepton mass [12] and is based upon a covariant form of the charged leptonic current with definite lepton helicity. In the present calculations, we use the same set of 18th interfering nucleon resonances with masses below $2 \text{ GeV}/c^2$ as in Ref. [8] but with all relevant input parameters updated according to the current data [7]. Significant factors (normalization coefficients etc.) estimated in Ref. [8] numerically are recalculated by using the new data and a more accurate integration algorithm.

The relativistic quark model of Feynman, Kislinger, and Ravndal [13] adopted in the RS approach unambiguously determines the structure of the transition amplitudes involved into the calculation and the only unknown structures are the vector and axial-vector transition form factors $G^{V,A}(Q^2)$. In Ref. [8] they are assumed to have the form

$$G^{V,A}(Q^2) \propto \left(1 + \frac{Q^2}{4M_N^2}\right)^{1/2-n} \left(1 + \frac{Q^2}{M_{V,A}^2}\right)^{-2} \quad (2)$$

with the ‘‘standard’’ value of the vector mass $M_V = 0.84 \text{ GeV}/c^2$ (that is the same as in the naive dipole parametrization of the elastic vector form factor) [14]. The axial mass $M_A = M_A^{\text{RES}}$ (which was fixed to be $0.95 \text{ GeV}/c^2$ in the basic model) will be a free parameter in the present study. The integer n in the first (‘‘ad hoc’’) factor of Eq. (2) is the number of oscillator quanta present in the final resonance.

To compensate for the difference between the SU_6 predicted value ($-5/3$) and the experimental value for the nucleon axial-vector coupling g_A , Rein and Sehgal introduced a renormalization factor $Z = 0.75$. In order to adjust the renormalization to the current world averaged value $g_A = -1.2695 \pm 0.0029$ [7] (assuming $g_V = 1$) we have adopted $Z = 0.762$.

Another essential ingredient of the RS approach is the nonresonance background (NRB) for which we use the ansatz suggested in Ref. [8]. The NRB contribution is important for description of the existing data on the reactions $\nu_\mu n \rightarrow \mu^- n \pi^+$, $\nu_\mu n \rightarrow \mu^- p \pi^0$, $\bar{\nu}_\mu p \rightarrow \mu^+ p \pi^-$, and $\bar{\nu}_\mu p \rightarrow \mu^+ n \pi^0$. Therefore it must be taken into account also in the RES contribution to the total cross section if $W_{\text{cut}}^{\text{RES}} \leq W_{\text{cut}}^{\text{DIS}}$. It is not so obvious for the opposite (and by no means unphysical) case, $W_{\text{cut}}^{\text{RES}} > W_{\text{cut}}^{\text{DIS}}$, since the DIS contribution partially accounts for the NRB. So, it would be natural in this case to consider the NRB as an additional ‘‘free parameter’’ of the likelihood analysis.

However, in this paper we pass over this complication and include the NRB contribution into all variants of the fit.

Figure 1 shows the RES contributions into the total CC cross sections (divided by neutrino energy) evaluated by using the extended RS model. In this example, we use $M_A^{\text{RES}} = 1.08 \text{ GeV}/c^2$, the best fit value obtained from the recent analysis of the BNL 7-foot bubble chamber deuterium experiment [15] (hereafter referred to as “BNL-2002”) based on the total event sample of 1.8 M pictures (held two periods of runs in 1976-77 and 1979-80). The curves in panels (b) and (c) are for the sums of the cross sections for the processes indicated in the legends. The solid and dashed curves in these panels correspond to the calculation with and without the NRB contributions, respectively. The calculations are done for the six values of the cutoff parameter $W_{\text{cut}}^{\text{RES}} = 1.2, 1.3, 1.4, 1.6, 1.8, 2.0 \text{ GeV}$; clearly the cross sections decrease with decreasing the cutoff.

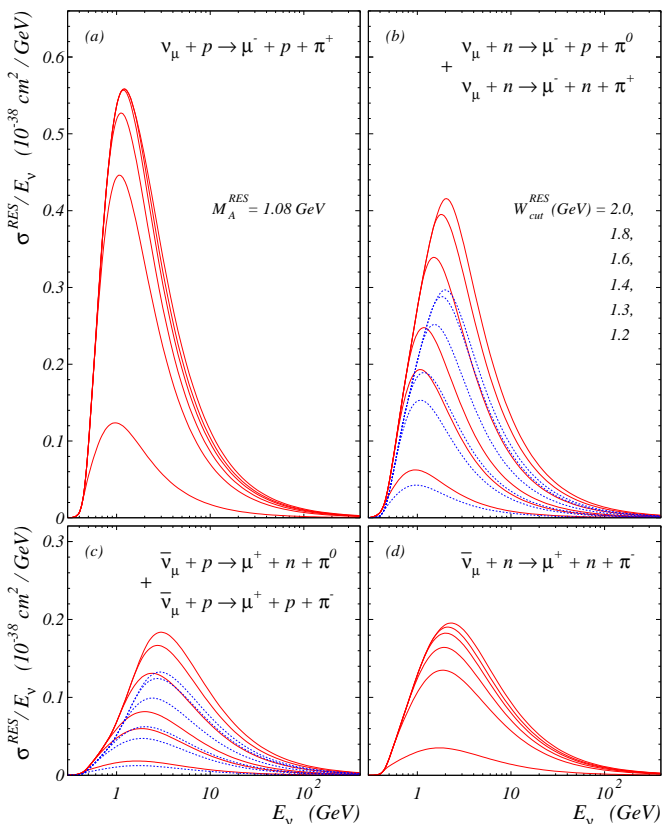


FIG. 1: The total CC single-pion production cross sections divided by neutrino energy evaluated with the extended RS model using $M_A^{\text{RES}} = 1.08 \text{ GeV}/c^2$ for the six values of the cutoff parameter $W_{\text{cut}}^{\text{RES}} = 1.2, 1.3, 1.4, 1.6, 1.8, 2.0 \text{ GeV}$ (from bottom to top curves in each panel). The solid and dashed curves correspond to the cross sections calculated with and without the NRB contributions, respectively.

The next and more substantial drawback of the present study is in neglecting the nuclear corrections for the RES (as well as for the DIS) contribution. A justification is

in the fact that these effects were subtracted in a certain part of the total cross section data while the necessary information is unavailable for another part of the data. We intend to remove this drawback in future study.

C. Deep inelastic scattering

The DIS CC $\nu_\mu N$ and $\bar{\nu}_\mu N$ differential cross sections are represented by the standard set of five structure functions $F_i = F_i(x, Q^2)$ (see, e.g., Refs. [16, 17]):

$$\frac{d^2\sigma_{\nu(\bar{\nu})}^{\text{DIS}}}{dx dy} = \frac{G_F^2 M_N E_\nu}{\pi(1 + Q^2/M_W^2)^2} \sum_{i=1}^5 A_i(x, y, E_\nu) F_i(x, Q^2), \quad (3)$$

where x and y are the usual DIS kinematic variables. The coefficient functions A_i are

$$\begin{aligned} A_1 &= y \left(xy + \frac{m_\mu^2}{2M_N E_\nu} \right), \\ A_2 &= 1 - \left(1 + \frac{M_N x}{2E_\nu} \right) y - \frac{m_\mu^2}{4E_\nu^2}, \\ A_3 &= \pm y \left[x \left(1 - \frac{y}{2} \right) - \frac{m_\mu^2}{4M_N E_\nu} \right], \\ A_4 &= \frac{m_\mu^2}{2M_N E_\nu} \left(y + \frac{m_\mu^2}{2M_N E_\nu x} \right), \\ A_5 &= -\frac{m_\mu^2}{M_N E_\nu}. \end{aligned} \quad (4)$$

The functions F_1 and F_2 are related through the measurable structure function $R = F_L/(2xF_1) = \sigma_L/\sigma_T$, the ratio of longitudinal and transverse cross sections in DIS:

$$\mathfrak{D}F_2 = 2xF_1, \quad \mathfrak{D} = \frac{1}{1+R} \left(1 + \frac{Q^2}{\nu^2} \right), \quad (5)$$

where $\nu = yE_\nu$. In order to satisfy Eq. (5) and, simultaneously, the collinear parton model (PM) limit that is the Callan-Gross relation ($F_2^{\text{PM}} \rightarrow 2xF_1^{\text{PM}}$ as $Q^2 \rightarrow \infty$ or $\mathfrak{D} \rightarrow 1$), the exact structure functions $F_{1,2}$ must be related to those in the PM limit, $F_{1,2}^{\text{PM}}$, as

$$F_1 = (1 - a + a\mathfrak{D}) F_1^{\text{PM}}, \quad F_2 = [a + (1 - a)/\mathfrak{D}] F_2^{\text{PM}}. \quad (6)$$

Till the function $a = a(x, Q^2)$ is not specified, these relations are the most general. There are two simplest limiting possibilities for a : $a = 0$ ($F_1 = F_1^{\text{PM}}$, $F_2 = F_2^{\text{PM}}/\mathfrak{D}$) and $a = 1$ ($F_1 = \mathfrak{D}F_1^{\text{PM}}$, $F_2 = F_2^{\text{PM}}$). Our analysis of the experimental data described in the next section and testing many models for the parton density functions (PDF) suggests that the “ $a = 1$ model” works quite satisfactory. Hereafter we will discuss just this particular case.

For the structure function R we use a combination of two up-to-date parametrizations: inside the nucleon resonance region $1.15 < W^2 < 3.9 \text{ GeV}^2$ and $0.3 < Q^2 <$

5.0 GeV² we apply the recent precision result of the Jefferson Lab Hall C E94-110 Collaboration [19, 20]; outside this region we apply the R_a version of the accurate 6-parameter fit to the world data on R proposed by the SLAC E-143 Collaboration [21]. The two parametrizations are sewn by a 2D B-spline in the boundary of the kinematic regions.

In Fig. 2 we show a comparison of the described model with the data from JLab [19] and the results of the σ_L and σ_T separation performed by Dress *et al.* [22] and based on the data of many older measurements of the ep cross sections in the resonance region. The filled bands in the figure are obtained by varying Q^2 within the ranges 0.18 – 1 GeV² (a), 1 – 2 GeV² (b), 2 – 3 GeV² (c), and 3 – 5 GeV² (d).

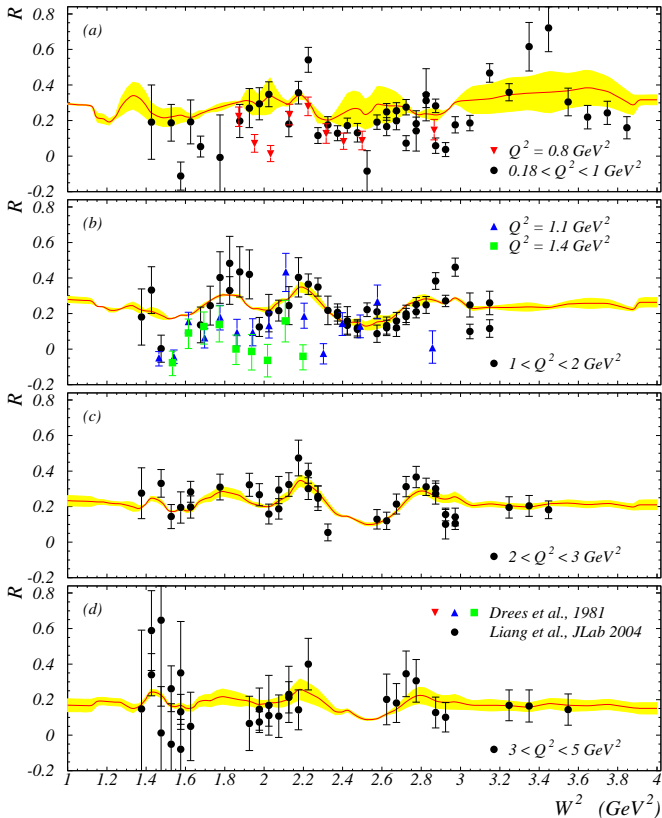


FIG. 2: The structure function $R = \sigma_L/\sigma_T$ vs. W^2 obtained by the Rosenbluth analysis of the inclusive ep cross sections measured at the JLab Hall C experiment [19] for the Q^2 ranges indicated in the panels. Also shown are the results of several earlier experiments on ep scattering in the resonance region converted to R in Ref. [22] for $Q^2 = 0.8$ (a), 1.1 and 1.4 GeV² (b). The bands are evaluated by using the model for R described in the text and by varying Q^2 within the corresponding ranges; the curves are for the R averaged over these ranges.

Since the JLab fit has been obtained from the data on ep scattering, we corrected it to the νN scattering and tested by using the QCD based Altarelli-Martinelli equation [23]. In fact, the difference between $R^{(e,\mu)}$ and

$R^{(\nu,\bar{\nu})}$ is practically negligible within the relevant kinematic region below the charm production threshold and small above the threshold.

From Eqs. (4) and the exact νN kinematics it follows that

$$A_4 < \frac{m_\mu^2}{2M_N E_\nu} \left(1 - \frac{m_\mu}{E_\nu}\right) < \frac{m_\mu}{2M_N} \quad \text{and} \quad |A_5| < \frac{m_\mu}{M_N}.$$

Due to this suppression and in view of the scale of the functions F_4 and F_5 followed from the NLO pQCD plus target mass calculations [16], the $A_4 F_4$ and $A_5 F_5$ terms in Eq. (3) can only be significant near the reaction threshold [18]. Hence the structure functions $F_{4,5}$ can be estimated roughly, by using the approximate relations valid in the PM limit with massless quarks:

$$F_4 \approx \frac{1}{2} \left(\frac{F_2}{2x} - F_1 \right) = \frac{1}{2} \left(\frac{1}{\mathcal{D}} - 1 \right) F_1$$

and

$$F_5 \approx \frac{F_2}{2x} = \frac{F_1}{\mathcal{D}}.$$

The PDF contributions into all structure functions are divided, in the standard fashion, onto “non charm production” (ncp) and “charm production” (cp) parts:

$$q^{\text{nCP}} = q^{\text{nCP}}(x_N, Q^2) \quad \text{and} \quad q^{\text{CP}} = q^{\text{CP}}(\xi, Q^2),$$

where $x_N = 2x / (1 + \sqrt{1 + Q^2/\nu^2})$ is the Nachtmann variable, $\xi = x_N (1 + m_c^2/Q^2)$ is the collinear limit of the light-cone variable with massless u , d , and s quarks, and $m_c = 1.3 \text{ GeV}/c^2$ is the mass of c quark. The b and t quark contributions are neglected.

We have tested several popular PDF models but in this paper we only discuss the results obtained with the latest version of CTEQ 6D NLO PDF set with four flavors (standard DIS scheme, version 6.12, December 14, 2004) [24].

Figure 3 shows the total DIS $\nu_\mu p$, $\nu_\mu n$, $\bar{\nu}_\mu p$, and $\bar{\nu}_\mu n$ CC cross sections divided by neutrino energy evaluated with the CTEQ 6D NLO PDFs for the five values of the cutoff parameter $W_{\text{cut}}^{\text{DIS}} = 1.2, 1.4, 1.6, 1.8,$ and 2.0 GeV ; Clearly, the cross sections increase with decreasing of the cutoff. Since the CTEQ 6D PDFs cannot be extrapolated to the exact kinematic boundaries, we have to freeze Q^2 below some value Q_f^2 . In Fig. 3, this value varies within the range 0.6 to 1.0 GeV² and the widths of the bands reflect the corresponding variations of the DIS cross sections. The Q_f dependence is in general nonmonotonic and diminishes with increasing the cutoff value. In the present likelihood analysis, the Q^2 variable is freezing below $Q_f^2 = 0.8 \text{ GeV}^2$. The error introduced by this approximation is estimated to be less than 1-2% that is small in comparison with the uncertainties of the experimental data and indetermination in other phenomenological parameters.

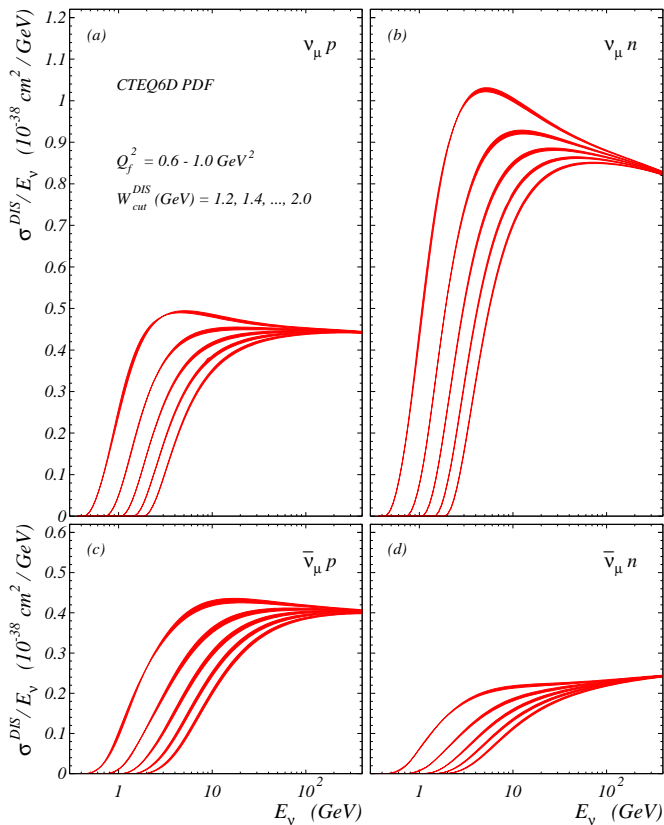


FIG. 3: The total DIS $\nu_\mu p$, $\nu_\mu n$, $\bar{\nu}_\mu p$, and $\bar{\nu}_\mu n$ CC cross sections divided by neutrino energy evaluated with the CTEQ 6D NLO PDFs for the five values of the cutoff parameter $W_{\text{cut}}^{\text{DIS}} = 1.2$ to 2.0 GeV from top to bottom with steps of 0.2 GeV. The widths of the bands correspond to variation of the freezing parameter Q_f^2 from 0.6 to 1.0 GeV^2 .

III. DATA SET

We have examined and classified all available experimental data on the QES and total CC νN and $\bar{\nu} N$ cross sections as well as independently measured relative quantities like the ratios $\sigma_{\nu n}/\sigma_{\nu p}$, $\sigma_{\bar{\nu} n}/\sigma_{\bar{\nu} p}$, $\sigma_{\bar{\nu} p}/\sigma_{\nu p}$, and so on. Published results from the relevant experiments at ANL [25, 26, 27, 28], BNL [29, 30, 31, 32, 33], FNAL [34, 35, 36, 37, 38, 39, 40, 41, 42, 43, 44, 45, 46, 47, 48, 49, 50, 51, 52, 53, 54, 55, 56] LANL [57], CERN [58, 59, 60, 61, 62, 63, 64, 65, 66, 67, 68, 69, 70, 71, 72, 73, 74, 75, 76, 77, 78, 79, 80, 81, 82, 83, 84, 85, 86, 87, 88], and IHEP [89, 90, 91, 92, 93, 94, 95, 96, 97, 98, 99] are included dating from the end of sixties to the present day, covering ν_μ , $\bar{\nu}_\mu$, ν_e , and $\bar{\nu}_e$ beams on a variety of hydrogen and nuclear targets, with energies from the thresholds to about 350 GeV. A detailed description of our database will be published elsewhere. Here we briefly depict the most important points.

Not all the collected data are involved into the analysis. We excluded from the fit:

- the experimental results which are undoubtedly ob-

solete, superseded or reconsidered (due to increased statistics, revised normalization, etc.) in the posterior reports of the same Collaborations;

- the datasets which are a transformation of the others derived from the same experimental samples (for instance, we used either the cross section σ or the “slope” σ/E_ν measured in the same experiment);
- the cross sections, slopes, and ratios averaged over a wide energy range when the energy-binned dataset is available.

We quenched a wish to reject the results seeming self-contradictory or being in obvious disagreement with the major dataset. A few exceptions and particular cases will be expounded in the next section.

If only the bounds of the energy bin were available, we either averaged the data (and the relevant calculated quantity) over the bin or estimated the mean energy from the (anti)neutrino beam spectrum (when the necessary information was accessible from the original paper or another description of the experiment). The statistical and systematic errors of the data were always summed up quadratically.

IV. LIKELIHOOD ANALYSIS

The four above-mentioned parameters M_A^{QES} , M_A^{RES} , $W_{\text{cut}}^{\text{RES}}$, and $W_{\text{cut}}^{\text{DIS}}$ involved into the merging of the QES, RES, and DIS contributions (Sect. II) were fitted to the described data by using the CERN function minimization and error analysis package “MINUIT” (version 94.1) [100]. In order to test validity of the dataset and the fitting procedure, we have examined many variants of 1-, 2-, 3-, and 4-parameter fits taking care of getting the correct correlation coefficients printed by MINUIT. Illustrative results of this analysis are listed in Tables I, II and III together with the obtained values of χ^2 per number of degrees of freedom (NDF). The number of significant digits shown in the last columns of Tables II and III is more than needed; we only keep these to clarify the χ^2 minima.

The first column in each table is for designation of different exercises of the fit. The numbers in bold-face correspond to the fixed trial values of the parameters used as inputs. The errors of the output parameters correspond to the usual one-standard-deviation (1σ) errors (MINUIT default) [101].

Visualization of the results is shown in Figs. 4–9 for the B3 variant of the fit which is preferable in our opinion.

Figure 4 shows the QES data from Refs. [25, 26, 27, 31, 47, 55, 57, 58, 59, 64, 69, 70, 87, 92, 93, 94, 95, 97, 98] together with the B3 best fit to the *full* set of the data satisfying the criteria described in Sect. III (NDF = $670 - 3 = 667$). The FNAL 1984 data points from Ref. [51] (neon-hydrogen target) are shown here only for a comparison.

TABLE I: One-parameter fits with the corresponding χ^2 per NDF = 669. Trial parameters are bold-faced.

Fit	M_A^{QES} (GeV)	M_A^{RES} (GeV)	$W_{\text{cut}}^{\text{RES}}$ (GeV)	$W_{\text{cut}}^{\text{DIS}}$ (GeV)	$\frac{\chi^2}{\text{NDF}}$
A1	0.8	1.08	1.47 ± 0.02		1.67
	0.9	1.08	1.50 ± 0.01		1.52
	1.0	1.08	1.53 ± 0.02		1.47
	1.1	1.08	1.56 ± 0.01		1.56
	1.2	1.08	1.58 ± 0.02		1.80
B1	0.8	2.0	1.47 ± 0.01		1.68
	0.9	2.0	1.52 ± 0.01		1.52
	1.0	2.0	1.58 ± 0.01		1.47
	1.1	2.0	1.64 ± 0.01		1.56
	1.2	2.0	1.71 ± 0.01		1.82

TABLE II: Two-parameter fits with the corresponding χ^2 per NDF = 668. Trial parameters are bold-faced.

Fit	M_A^{QES} (GeV)	M_A^{RES} (GeV)	$W_{\text{cut}}^{\text{RES}}$ (GeV)	$W_{\text{cut}}^{\text{DIS}}$ (GeV)	$\frac{\chi^2}{\text{NDF}}$
A2	0.99 ± 0.02	1.08	1.53 ± 0.02		1.469
B2	0.96 ± 0.01		1.31 ± 0.01	1.4	1.484
C2	0.8	1.11 ± 0.08	1.28 ± 0.01	1.4	1.631
	0.9	1.10 ± 0.08	1.28 ± 0.01	1.4	1.499
	1.0	1.09 ± 0.07	1.28 ± 0.01	1.4	1.493
	1.1	1.08 ± 0.07	1.28 ± 0.01	1.4	1.635
	1.2	1.07 ± 0.06	1.29 ± 0.01	1.4	1.943
D2	0.8	0.91 ± 0.04	1.41 ± 0.02		1.649
	0.9	0.97 ± 0.04	1.46 ± 0.02		1.507
	1.0	1.03 ± 0.04	1.51 ± 0.02		1.468
	1.1	1.07 ± 0.04	1.55 ± 0.02		1.558
	1.2	1.10 ± 0.04	1.59 ± 0.02		1.801
E2	0.8	1.00 ± 0.04	2.0	1.53 ± 0.02	1.651
	0.9	1.04 ± 0.04	2.0	1.57 ± 0.02	1.505
	1.0	1.08 ± 0.04	2.0	1.61 ± 0.02	1.469
	1.1	1.11 ± 0.04	2.0	1.65 ± 0.02	1.566
	1.2	1.14 ± 0.04	2.0	1.68 ± 0.02	1.814
F2	0.8	1.08	1.28 ± 0.01	1.38 ± 0.01	1.629
	0.9	1.08	1.77 ± 0.09	1.56 ± 0.02	1.500
	1.0	1.08	1.70 ± 0.14	1.57 ± 0.03	1.465
	1.1	1.08	1.34 ± 0.03	1.49 ± 0.01	1.551
	1.2	1.08	1.37 ± 0.04	1.53 ± 0.02	1.787

They are not included into the fit since were obtained by a recalculation from the DIS data (included into the fit, see Fig. 5) by using a prescription given in Ref. [51] and the errors for these points were estimated approximately. In order to facilitate comparison, the data points for the experiments performed with the nuclear targets different from D_2 and Ne-H_2 are converted to a free nucleon target [102]. The nuclear effects for the deuterium [26, 27, 31, 47, 87], neon-hydrogen [51] and averaged iron data [55] (shown in Fig. 4 by filled rectangles) were subtracted by the authors of the experiments. The curves are calculated with $M_A^{\text{QES}} = 0.98 \text{ GeV}/c^2$, the

TABLE III: Three- and four-parameter fits with the corresponding χ^2 per NDF (= 667 and 666, respectively). Trial parameters are bold-faced.

Fit	M_A^{QES} (GeV)	M_A^{RES} (GeV)	$W_{\text{cut}}^{\text{RES}}$ (GeV)	$W_{\text{cut}}^{\text{DIS}}$ (GeV)	$\frac{\chi^2}{\text{NDF}}$
A3	0.93 ± 0.01	1.06 ± 0.07	1.27 ± 0.01	1.35	1.542
	0.95 ± 0.01	1.09 ± 0.08	1.28 ± 0.01	1.40	1.481
	0.98 ± 0.01	1.13 ± 0.08	1.30 ± 0.02	1.45	1.461
	0.98 ± 0.02	1.00 ± 0.03	1.55 ± 0.04	1.50	1.467
	0.98 ± 0.02	1.05 ± 0.03	1.69 ± 0.07	1.55	1.463
B3	0.98 ± 0.02	1.02 ± 0.04	1.50 ± 0.02		1.468
C3	0.98 ± 0.01	1.01 ± 0.03	1.50	1.50 ± 0.00	1.468
	0.98 ± 0.02	1.02 ± 0.04	1.55	1.51 ± 0.02	1.466
	0.98 ± 0.02	1.03 ± 0.04	1.60	1.53 ± 0.02	1.464
	0.98 ± 0.02	1.04 ± 0.04	1.65	1.54 ± 0.02	1.463
	0.98 ± 0.02	1.05 ± 0.04	1.70	1.55 ± 0.02	1.463
	0.98 ± 0.02	1.06 ± 0.04	1.75	1.56 ± 0.02	1.464
	0.98 ± 0.02	1.06 ± 0.04	1.80	1.57 ± 0.02	1.464
	0.98 ± 0.02	1.06 ± 0.04	1.85	1.58 ± 0.02	1.465
	0.98 ± 0.02	1.07 ± 0.04	1.90	1.59 ± 0.02	1.467
	0.98 ± 0.02	1.07 ± 0.04	1.95	1.59 ± 0.02	1.468
0.98 ± 0.02	1.07 ± 0.04	2.00	1.60 ± 0.02	1.469	
D3	0.98 ± 0.01	1.08	1.73 ± 0.26	1.57 ± 0.05	1.464
E3	0.8	1.10 ± 0.08	1.28 ± 0.01	1.38 ± 0.01	1.631
	0.9	1.11 ± 0.08	1.29 ± 0.02	1.42 ± 0.01	1.497
	1.0	1.13 ± 0.08	1.30 ± 0.02	1.46 ± 0.01	1.463
	1.1	1.17 ± 0.06	1.31 ± 0.02	1.50 ± 0.01	1.551
1.2	1.19 ± 0.06	1.32 ± 0.02	1.53 ± 0.01	1.783	
A4	0.98 ± 0.02	1.13 ± 0.08	1.30 ± 0.02	1.45 ± 0.01	1.463

value obtained from the global B3 fit. The grey bands show the standard deviation from the best-fit cross sections due to the error of $0.02 \text{ GeV}/c^2$ in determination of M_A^{QES} . Note that the best-fit value of M_A^{QES} is in agreement with that obtained by a single-parameter fit to the QES data only, $M_A^{\text{QES}} = 0.94 \pm 0.04 \text{ GeV}/c^2$.

The obtained value of M_A^{QES} , being lower, does not contradict to the latest (still preliminary) result by the K2K experiment [103]

$$M_A^{\text{QES}}(\text{K2K}) = 1.06 \pm 0.03 (\text{stat.}) \pm 0.14 (\text{syst.}) \text{ GeV}/c^2.$$

It is however essentially below the value of $1.1 \text{ GeV}/c^2$ used in the recent atmospheric neutrino oscillation analysis of the Super-Kamiokande I experiment [104].

In Figs. 5 and 6 we collect the main subset of the experimental data on the total CC cross sections and their slopes for an isoscalar nucleon (hereafter denoted by N) from Refs. [28, 33, 36, 38, 41, 51, 60, 62, 62, 66, 72, 73, 90] and [28, 30, 33, 34, 36, 38, 41, 45, 46, 48, 49, 51, 52, 53, 56, 60, 62, 71, 72, 73, 75, 76, 78, 81, 85, 86, 89, 90, 91, 99], respectively. The majority of these data is included into the fit. The curves and bands show the QES, RES, and DIS contributions (Fig. 6) and their sums (both figures) calculated with the best-fitted values of M_A^{QES} , M_A^{RES} , and $W_{\text{cut}}^{\text{RES}} = W_{\text{cut}}^{\text{DIS}}$ (the latter equality is the restriction used in the B3 fit).

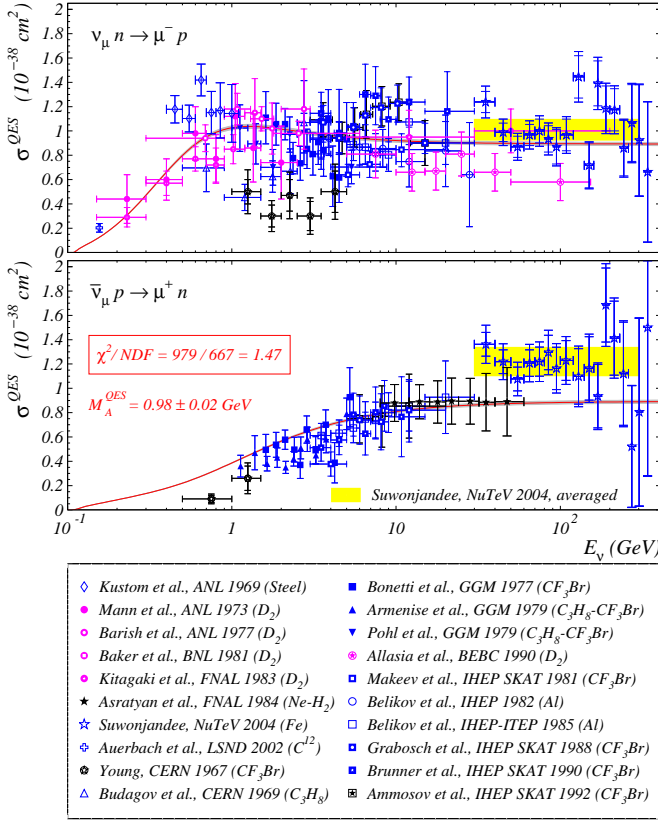


FIG. 4: Total QES cross sections measured by the experiments ANL 1969 [25], ANL 1973 [26], ANL 1977 [27], BNL 1981 [31], FNAL 1983 [47], FNAL 1984 [51], NuTeV 2004 [55], LSND 2002 [57], CERN 1967 [58], CERN 1969 [59], GGM (Gargamelle) 1977 [64], GGM 1979 [69, 70], BEBC 1990 [87], IHEP SKAT 1981 [92], IHEP 1982 [93], IHEP-ITEP 1985 [94], IHEP SKAT 1988 [95], IHEP SKAT 1990 [97], and IHEP SKAT 1992 [98]. Both statistical and total errors are shown for the earliest low-energy data of CERN [58] (excluded from the fit) and for the most current high-energy data of NuTeV [55]. The filled rectangles are for the NuTeV data (with the total error) averaged over the wide energy range 30 to 300 GeV. The data for nuclear targets (indicated in the parentheses in the legend) are converted to a free nucleon. The curves are for the QES cross sections calculated with the value of $M_A^{QES} = 0.98 \text{ GeV}/c^2$ obtained from the global B3 fit (see text). The narrow grey bands show the standard 1σ deviation from the best-fit curves.

Figure 7 accumulates the data on the cross section ratios $\sigma_{\bar{\nu}_\mu N}/\sigma_{\nu_\mu N}$ and $\sigma_{\bar{\nu}_e N}/\sigma_{\nu_e N}$ (isoscalar target) according to Refs. [35, 36, 37, 39, 41, 54, 56, 62, 63, 65, 66, 68, 71, 75, 77, 81, 84, 85, 89, 91, 99]. The paper [66] supersedes the earlier publications of the Gargamelle Collaboration [63] (shown by filled rectangle) and [68]. The major part of these data is obtained from the cross sections measured in the same experiments. The other, like the recent NuTeV result [56], correspond to a wide energy range with no indication of the mean energy. Due to these and similar reasons all these data are excluded from

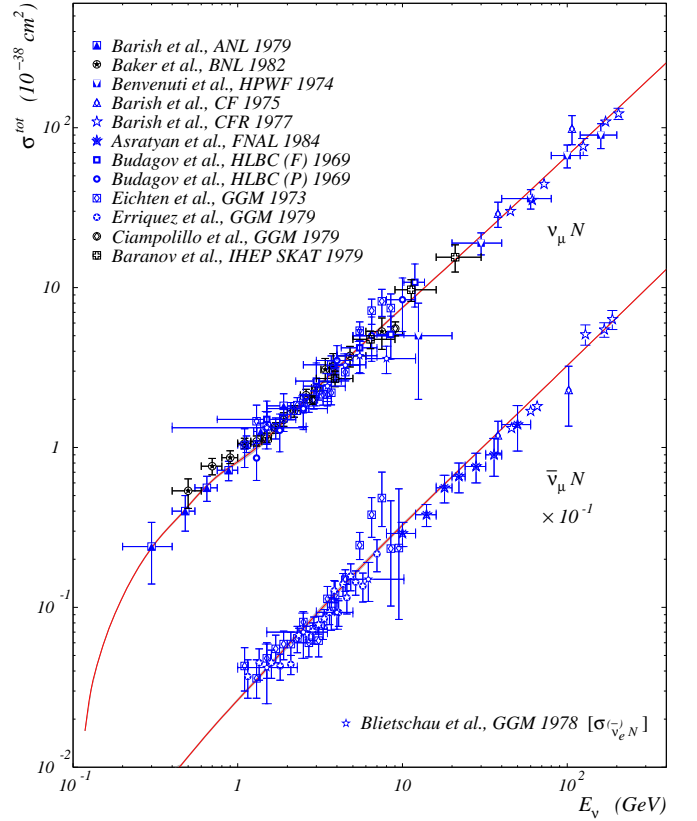


FIG. 5: Total CC cross sections for ν_μ and $\bar{\nu}_\mu$ scattering off an isoscalar nucleon measured by the experiments ANL 1979 [28], BNL 1982 [33], HPWF 1974 [36], CF 1975 [38], CFR 1977 [41], FNAL 1984 [51], HLBC 1969 (freon, 1963-64 and propane, 1967 runs) [60], GGM 1973 [62], GGM 1979 [72, 73], and IHEP SKAT 1979 [90]. Also shown are the $\nu_e N$ and $\bar{\nu}_e N$ cross sections measured by the GGM 1978 experiment [66]. The antineutrino data are scaled with a factor of 0.1 for better visualization. The curves and bands show the cross sections calculated with the best-fitted values of M_A^{QES} , M_A^{RES} , and $W_{cut}^{RES} = W_{cut}^{DIS}$ (see text and legend in Fig. 6).

the analysis and only shown here for a comparison with the result of the global B3 fit. The cross section ratios $\sigma_{\nu n}/\sigma_{\nu p}$ and $\sigma_{\bar{\nu} n}/\sigma_{\bar{\nu} p}$ from Refs. [28, 32, 33, 40, 43, 44, 50, 61, 67, 72, 74, 79, 80, 81, 88, 96] are shown in Fig. 8. The results of Refs. [33, 40, 61, 79, 81] are excluded from the fit due to the reasons mentioned in Sect. III. The near-threshold point from Ref. [32] is removed since its deviation from the theoretical prediction is unphysically high. Six panels of Fig. 9 show the data of different kinds from Refs. [28, 29, 33, 42, 79, 80, 81, 83]. Almost all data points participate in the analysis. The curves and bands in Figs. 7, 8, and 9 are calculated with the parameters obtained from the global B3 fit (see legend in Fig. 6).

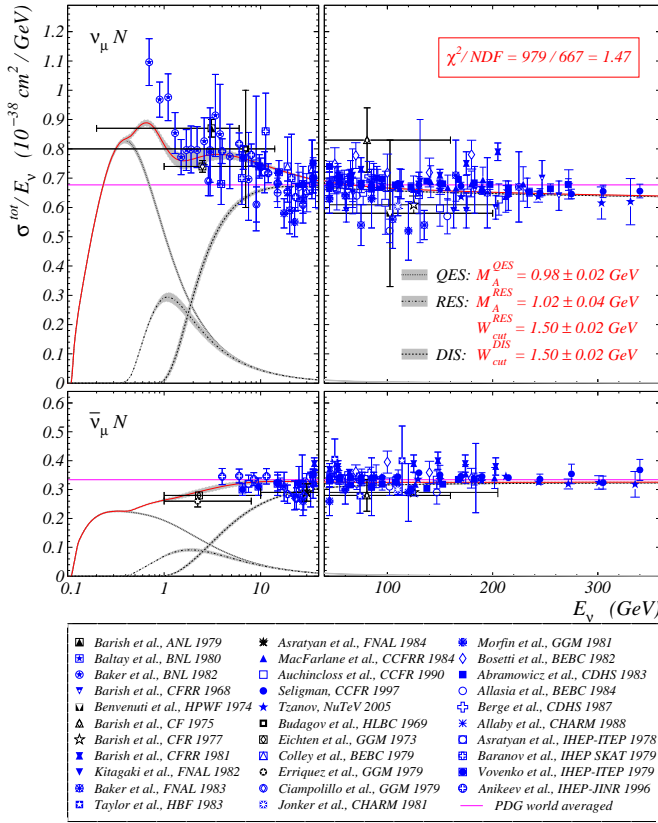


FIG. 6: Slopes of the total CC cross sections for $\nu_\mu N$ and $\bar{\nu}_\mu N$ scattering off an isoscalar nucleon measured by the experiments ANL 1979 [28], BNL 1980 [30], BNL 1982 [33], CFRR 1968 [34], HPWF 1974 [36], CF 1975 [38], CFRR 1977 [41], CFRR 1981 [45], FNAL 1982 [46], FNAL 1983 [48], HBF 1983 [49], FNAL 1984 [51], CCFRR 1984 [52], CCFR 1990 [53], CCFR 1997 [54], NuTeV 2005 [56], HLBC 1969 [60], GGM 1973 [62], BEBC 1979 [71], GGM 1979 [72, 73], CHARM 1981 [75], GGM 1981 [76], BEBC 1982 [77], CDHS 1983 [78], BEBC 1984 [81], CDHS 1987 [85], CHARM 1988 [86], IHEP-ITEP 1978 [89], IHEP SKAT 1979 [90], IHEP-ITEP 1979 [91], and IHEP-JINR 1996 [99]. The data points with horizontal error bars are for the slopes averaged over the wide energy ranges; these do not participate in the fit and the corresponding energy binned data (included into the fit) are shown in Fig. 5. The curves and bands show the QES, RES, and DIS contributions and their sums calculated with the best-fitted values of the parameters depicted in the legend in top panel. The averaged values over all energies $(0.677 \pm 0.014) \times 10^{-38} \text{ cm}^2/\text{GeV}$ (for $\nu_\mu N$) and $(0.334 \pm 0.008) \times 10^{-38} \text{ cm}^2/\text{GeV}$ (for $\bar{\nu}_\mu N$) obtained by the Particle Data Group [105] from the data by the experiments in Refs. [52, 53, 54, 85] are also shown (straight lines).

V. SUMMARY

Our analysis of the world neutrino data on the QES and total CC cross sections yields several thought-provoking conclusions. As is seen from Tables I, II, and

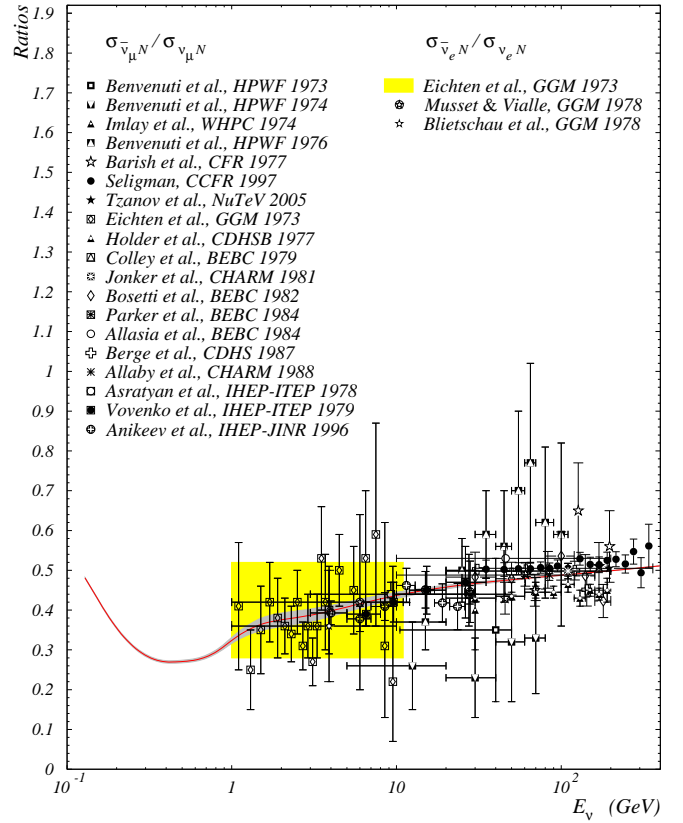


FIG. 7: The ratio $\sigma_{\bar{\nu}_\mu N}/\sigma_{\nu_\mu N}$ for an isoscalar nucleon measured by the experiments HPWF 1973 [35], HPWF 1974 [36], WHPC 1974 [37], HPWF 1976 [39], CFR 1977 [41], CCFR 1997 [54], NuTeV 2005 [56], GGM 1973 [62], CDHSB 1977 [65], BEBC 1979 [71], CHARM 1981 [75], BEBC 1982 [77] (revised according to Ref. [82]), BEBC 1984 [80, 81], CDHS 1987 [85], CHARM 1988 [84], IHEP-ITEP 1978 [89], IHEP-ITEP 1979 [91], and IHEP-JINR 1996 [99]. The ratio $\sigma_{\bar{\nu}_\mu N}/\sigma_{\nu_\mu N}$ reported in the three publications of the Gargamelle collaboration [63, 66, 68] is also shown. The curve and band are calculated with the same values of the fitted parameters as in Fig. 6.

III, in all variants of the fit there is a distinct minimum of χ^2 for M_A^{QES} around the “canonical” value of 1 GeV/c^2 with deviations $\lesssim 2\%$. This is mainly an effect of the QES data subset whose exclusion from the analysis would lead to an essential increase of M_A^{QES} for all variants (for example, in the B3 and A4 fits M_A^{QES} becomes equal to 1.13 ± 0.03 and $1.17 \pm 0.03 \text{ GeV}/c^2$, respectively).

The situation with the M_A^{RES} best-fit value is less definite: in different variants of the fit it fluctuates from about 1.00 to about 1.15 GeV/c^2 . This spread comprises the BNL-2002 results for M_A^{RES} [15] obtained with different approaches and does not contradict to the exact equality $M_A^{\text{RES}} = M_A^{\text{QES}}$. However, the 3- and 4-parameter fits favour the case $M_A^{\text{RES}} > M_A^{\text{QES}}$. Our “favorable” B3 variant of the fit yields the following values

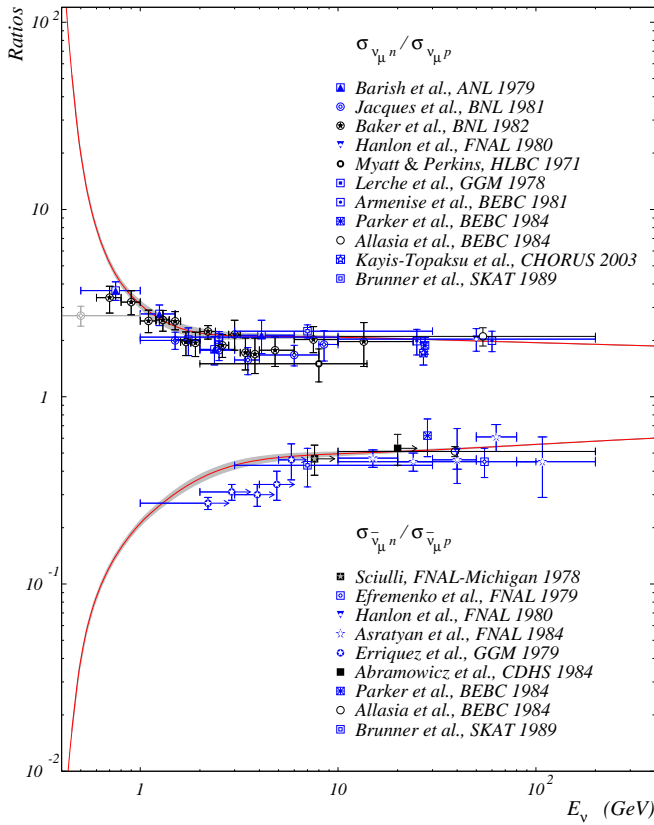


FIG. 8: The ratios $\sigma_{\nu n}/\sigma_{\nu p}$ and $\sigma_{\bar{\nu}n}/\sigma_{\bar{\nu}p}$ measured by the experiments ANL 1979 [28], BNL 1981 [32], BNL 1982 [33], FNAL-Michigan 1978 [40], FNAL 1979 [43], FNAL 1980 [44], FNAL 1984 [50], HLBC 1971 [61], GGM 1978 [67], GGM 1979 [72], BEBC 1981 [74], CDHS 1984 [79], BEBC 1984 [80, 81], CHORUS 2003 [88], and IHEP SKAT 1989 [96]. The data point of CDHS 1984 is recalculated in Ref. [50] from the ratio $\sigma_{\bar{\nu}p}/\sigma_{\bar{\nu}N}$. The curves and bands are calculated with the same values of the fitted parameters as in Fig. 6.

of the axial masses:

$$M_A^{\text{QES}} = 0.98 \pm 0.02 \text{ GeV}/c^2$$

and

$$M_A^{\text{RES}} = 1.02 \pm 0.04 \text{ GeV}/c^2.$$

The shape of the total and (all the more so) differential νN and $\bar{\nu}N$ cross sections is very sensitive to the values of the cutoff parameters $W_{\text{cut}}^{\text{RES}}$ and $W_{\text{cut}}^{\text{DIS}}$. From our analysis we have to conclude that these parameters cannot be fine-tuned with the confidence level sufficient for the current and future experiments for neutrino oscillations and related phenomena. However, the most worth-while versions of the fit indicate that $W_{\text{cut}}^{\text{RES}} \approx W_{\text{cut}}^{\text{DIS}}$ must be essentially above the value of 1.4 GeV approved in the data processing of many accelerator and astrophysical neutrino experiments. The outcome of the B3 fit is

$$W_{\text{cut}}^{\text{RES}} = W_{\text{cut}}^{\text{DIS}} = 1.50 \pm 0.02 \text{ GeV}.$$

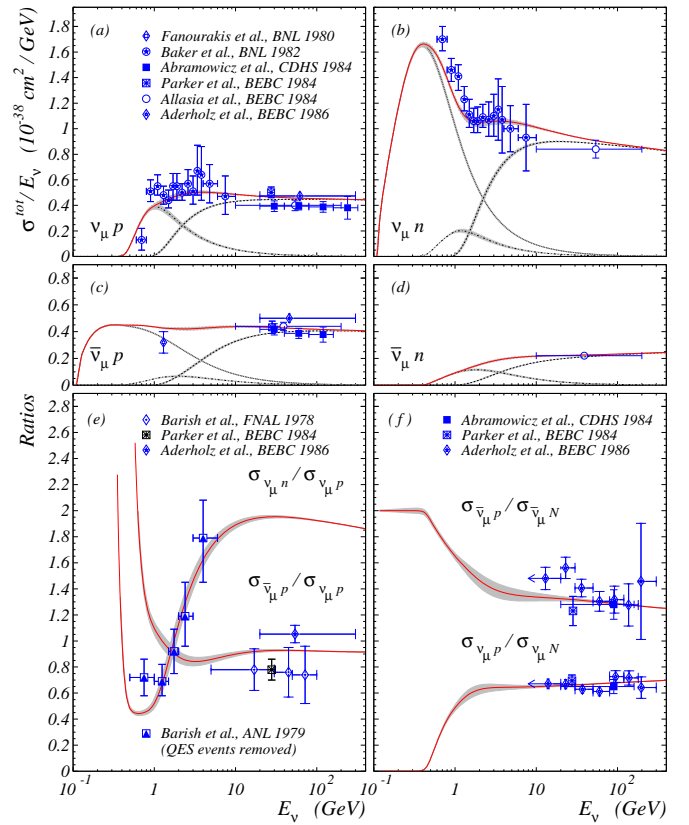


FIG. 9: (a), (b), (c), (d) – the slopes of the $\nu_{\mu}p$, $\nu_{\mu}n$, $\bar{\nu}_{\mu}p$, and $\bar{\nu}_{\mu}n$ total CC cross sections measured by the experiments BNL 1980 [29], BNL 1982 [33], CDHS 1984 [79], BEBC 1984 [80, 81], and BEBC 1986 [83]; (e) – the ratios $\sigma_{\nu n}/\sigma_{\nu p}$ (with quasielastic events removed) and $\sigma_{\bar{\nu}n}/\sigma_{\bar{\nu}p}$ measured by the experiments ANL 1979 [28], FNAL 1978 [42], BEBC 1984 [80], and BEBC 1986 [83]; (f) – the ratios $\sigma_{\nu p}/\sigma_{\nu N}$ and $\sigma_{\bar{\nu}p}/\sigma_{\bar{\nu}N}$ measured by the experiments CDHS 1984 [79], BEBC 1984 [80], and BEBC 1986 [83]. The curves and bands in all six panels are calculated with the same values of the fitted parameters as in Fig. 6.

Being considered deliberately, such a high value of the cutoff parameter for DIS puts forward the difficult problem of a correct accounting for the reactions of exclusive multi-hadron neutrino production and coherent neutrino-nucleus scattering.

Finally we have to note that the above conclusions are only valid for the theoretical models of the RES reactions, DIS structure functions and PDF, as well as the approximations and simplifications (sometimes risky) adopted in the present analysis. Investigation of alternative models, a more accurate treatment of the nuclear effects, and incorporation of additional experimental data is the matter of a forthcoming work.

Acknowledgments

We are grateful to the Physics Department of Florence University and Theoretical Department of KEK for warm hospitality during important stages of this work. We thank to Yongguang Liang and Martin Tzanov for providing us with the latest experimental data and relevant computer codes from JLab and NuTeV. We also thank to Kaoru Hagiwara, Sergey Kruchinin, Kentarou Mawatari, Dmitry Naumov, Roberto Petti, Gregory Vereshkov, and Hiroshi Yokoya for stimulating discussions.

-
- [1] V. Bernard, L. Elouadrhiri, and Ulf-G. Meißner, *J. Phys. G* **28**, R1 (2002) [hep-ph/0107088].
- [2] C. H. Llewellyn Smith, *Phys. Rept.* **3** C, 261 (1972).
- [3] M. F. Gari and W. Krümpelmann, *Phys. Lett. B* **274**, 159 (1992); **282**, 483 (E) (1992).
- [4] E. L. Lomon, *Phys. Rev. C* **66**, 045501 (2002) [nucl-th/0203081].
- [5] H. Budd, A. Bodek, and J. Arrington, hep-ex/0308005; *Nucl. Phys. B (Proc. Suppl.)* **139**, 90 (2005) [hep-ex/0410055].
- [6] Proceedings of the 10th International Conference on the Structure of Baryons, October 25–29, 2004, Palaiseau, France, edited by M. Guidal *et al.*, *Nucl. Phys. A* **755** (2005).
- [7] S. Eidelman *et al.* (Particle Data Group), *Phys. Lett. B* **592**, 1 (2004).
- [8] D. Rein and L. M. Sehgal, *Annals Phys.* **133**, 79 (1981).
- [9] D. Rein, *Z. Phys. C* **35**, 43 (1987).
- [10] K. S. Kuzmin, V. V. Lyubushkin, and V. A. Naumov, *Mod. Phys. Lett. A* **19**, 2815 (2004); *Phys. Part. Nucl.* **35**, S133 (2004) [hep-ph/0312107].
- [11] K. S. Kuzmin, V. V. Lyubushkin, and V. A. Naumov, *Nucl. Phys. B (Proc. Suppl.)* **139**, 158 (2005) [hep-ph/0408106].
- [12] As well as the final lepton spin, which is, however, not substantial to the present study.
- [13] R. P. Feynman, M. Kislinger, and F. Ravndal, *Phys. Rev. D* **3**, 2706 (1971); F. Ravndal, *Nuovo Cim.* **18** A, 385 (1973).
- [14] Considering that there are no solid reasons for choosing $M_V = 0.84 \text{ GeV}/c^2$, the parameter M_V is a natural candidate to be on the list of free parameters in a refined likelihood analysis involving the experimental data on the single-pion neutrino production.
- [15] K. Furuno *et al.*, a talk at the 2nd International Workshop on Neutrino-Nucleus Interactions in the Few GeV Region (“NUINT’02”), Irvine, California, December 12–15, 2002; RCNS-03-01, KEK Preprint 2003-48, September, 2003 (unpublished).
- [16] S. Kretzer and M. H. Reno, *Phys. Rev. D* **66**, 113007 (2002) [hep-ph/0208187].
- [17] S. Kretzer and M. H. Reno, *Phys. Rev. D* **69**, 034002 (2004) [hep-ph/0307023].
- [18] Not the case for the $\nu_\tau N$ and $\bar{\nu}_\tau N$ DIS processes.
- [19] Y. Liang *et al.*, nucl-ex/0410027; Y. Liang, Ph.D. Thesis, The American University, Washington, 2003. The detailed data of the JLab Hall C experiment are available at the URL: <http://www.jlab.org/~y10094a/E94110/e94110.html>.
- [20] The fit to the JLab data on R is based on a reparametrization of R_b model of the SLAC E-143 Collaboration [21]; Y. Liang (private communication, May, 2005).
- [21] K. Abe *et al.*, *Phys. Lett. B* **452**, 194 (1999) [hep-ex/9808028].
- [22] J. Dress, B. Gerhardt, Ch. Gerhardt, and A. Schneider, *Z. Phys. C* **7**, 183 (1981).
- [23] G. Altarelli and G. Martinelli, *Phys. Lett. B* **76**, 89 (1978); A. M. Cooper-Sarkar, R. C. E. Devenish, and A. De Roeck, *Int. J. Mod. Phys. A* **13**, 3385 (1998) [hep-ph/9712301].
- [24] J. Pumplin *et al.*, *JHEP* **207**, 012 (2002) [hep-ph/0201195]; S. Kretzer *et al.*, *Phys. Rev. D* **69**, 114005 (2004) [hep-ph/0307022]. The computer code is available at the URL: <http://user.pa.msu.edu/wkt/cteq/cteq6/cteq6pdf.html>.
- [25] R. L. Kustom *et al.*, *Phys. Rev. Lett.* **22**, 1014 (1969).
- [26] W. A. Mann *et al.*, *Phys. Rev. Lett.* **31**, 844 (1973).
- [27] S. J. Barish *et al.*, *Phys. Rev. D* **16**, 3103 (1977).
- [28] S. J. Barish *et al.*, *Phys. Rev. D* **19**, 2521 (1979).
- [29] G. Fanourakis *et al.*, *Phys. Rev. D* **21**, 562 (1980).
- [30] C. Baltay *et al.*, *Phys. Rev. Lett.* **44**, 916 (1980).
- [31] N. J. Baker *et al.*, *Phys. Rev. D* **23**, 2499 (1981).
- [32] P. F. Jacques *et al.*, *Phys. Rev. D* **24**, 1067 (1981).
- [33] N. J. Baker *et al.*, *Phys. Rev. D* **25**, 617 (1982).
- [34] B. C. Barish *et al.*, CALT 68-734, California Institute of Technology, Pasadena, 1968 (unpublished).
- [35] A. C. Benvenuti *et al.*, *Phys. Rev. Lett.* **30**, 1084 (1973).
- [36] A. C. Benvenuti *et al.*, *Phys. Rev. Lett.* **32**, 125 (1974).
- [37] R. Imlay *et al.*, Proceedings of the 17th International Conference on High Energy Physics, London, 1974, edited by J. R. Smith (Rutherford High Energy Laboratory, Chilton, 1975), p. V-50.
- [38] B. C. Barish *et al.*, *Phys. Rev. Lett.* **35**, 1316 (1975).
- [39] A. Benvenuti *et al.*, *Phys. Rev. Lett.* **37**, 189 (1976).
- [40] F. Sciulli, Proceedings of the Topical Conference on Neutrino Physics at Accelerators, Oxford, England, July 4-7, 1978, edited by A. G. Michette and P. B. Renton (Rutherford High Energy Laboratory, Chilton, 1978), p. 405.
- [41] B. C. Barish *et al.*, *Phys. Rev. Lett.* **39**, 1595 (1977).
- [42] B. C. Barish, *Phys. Rept.* **39**, 279 (1978).
- [43] V. I. Efremenko *et al.*, *Phys. Lett. B* **84**, 511 (1979).
- [44] J. Hanlon *et al.*, *Phys. Rev. Lett.* **45**, 1817 (1980).
- [45] B. Barish *et al.*, Proceedings of the 9th SLAC Summer Institute on Particle Physics “Strong Interactions”, Stanford, 1981, edited by A. Mosher (Stanford Linear Accelerator Center, Stanford, 1981), p. 641.
- [46] T. Kitagaki *et al.*, *Phys. Rev. Lett.* **49**, 98 (1982).
- [47] T. Kitagaki *et al.*, *Phys. Rev. D* **28**, 436 (1983).
- [48] N. J. Baker *et al.*, *Phys. Rev. Lett.* **51**, 735 (1983).
- [49] G. N. Taylor *et al.*, *Phys. Rev. Lett.* **51**, 739 (1983).
- [50] A. E. Asratyan *et al.*, ITEP-187, Institute of Experimental and Theoretical Physics, Moscow, 1984 (unpublished).
- [51] A. E. Asratyan *et al.*, *Yad. Fiz.* **39**, 619 (1984) [*Sov. J. Nucl. Phys.* **39**, 392 (1984)]; *Phys. Lett. B* **137**, 122 (1984).
- [52] D. MacFarlane *et al.*, *Z. Phys. C* **26**, 1 (1984).
- [53] P. S. Auchincloss *et al.*, *Z. Phys. C* **48**, 411 (1990).
- [54] W. G. Seligman, Ph.D. Thesis, Columbia University, New York, 1996; Nevis Report No. 292; FERMILAB-THESIS-1997-21, Fermi National Accelerator Laboratory, Illinois, 1997.
- [55] N. Suwonjandee, Ph.D. Thesis, University of Cincinnati, Cincinnati, 2004; FERMILAB-THESIS-2004-67, Fermi National Accelerator Laboratory, Illinois, 2004.
- [56] M. Tzanov *et al.* (NuTeV Collaboration), hep-ex/0509010; M. Tzanov (private communication, September, 2005).
- [57] L. B. Auerbach *et al.* (LSND Collaboration), *Phys. Rev. C* **66**, 015501 (2002) [nucl-ex/0203011].

- [58] E. C. M. Young, CERN “Yellow Report” CERN 67-12, European Organization for Nuclear Research, Geneva, 1967 (unpublished).
- [59] I. Budagov *et al.*, *Lett. Nuovo Cim.* **2**, 689 (1969).
- [60] I. Budagov *et al.*, *Phys. Lett. B* **30**, 364 (1969).
- [61] G. Myatt and D. H. Perkins, *Phys. Lett. B* **34**, 542 (1971).
- [62] T. Eichten *et al.*, *Phys. Lett. B* **46**, 274 (1973).
- [63] T. Eichten *et al.*, *Phys. Lett. B* **46**, 281 (1973).
- [64] S. Bonetti *et al.*, *Nuovo Cim.* **38 A**, 260 (1977).
- [65] M. Holder *et al.*, *Phys. Rev. Lett.* **39**, 433 (1977).
- [66] J. Blietschau *et al.* (Gargamelle Collaboration), *Nucl. Phys. B* **133**, 205 (1978).
- [67] W. Lerche *et al.* (Gargamelle Neutrino Propane Collaboration), *Nucl. Phys. B* **142**, 65 (1978).
- [68] P. Musset and J.-P. Vialle, *Phys. Rept.* **39**, 1 (1978).
- [69] N. Armenise *et al.*, *Nucl. Phys. B* **152**, 365 (1979).
- [70] M. Pohl *et al.* (Gargamelle Neutrino Propane Collaboration), *Lett. Nuovo Cim.* **26**, 332 (1979).
- [71] D. C. Colley *et al.*, *Z. Phys. C* **2**, 187 (1979).
- [72] O. Erriquez *et al.*, *Phys. Lett. B* **80**, 309 (1979).
- [73] S. Ciampolillo *et al.* (Gargamelle Neutrino Propane Collaboration and Aachen-Brussels-CERN-Ecole Polytechnique-Orsay-Padova Collaboration), *Phys. Lett. B* **84**, 281 (1979).
- [74] N. Armenise *et al.* (BEBC TST Neutrino Collaboration), *Phys. Lett. B* **102**, 374 (1981).
- [75] M. Jonker *et al.* (CHARM Collaboration), *Phys. Lett. B* **99**, 265 (1981); **100**, 521 (E) (1981); **103**, 469 (E) (1981).
- [76] J. G. Morfin *et al.*, *Phys. Lett. B* **104**, 235 (1981).
- [77] P. C. Bosetti *et al.* (Aachen-Bonn-CERN-Demokritos-London-Oxford-Saclay Collaboration), *Phys. Lett. B* **110**, 167 (1982).
- [78] H. Abramowicz *et al.*, *Z. Phys. C* **17**, 283 (1983).
- [79] H. Abramowicz *et al.*, *Z. Phys. C* **25**, 29 (1984).
- [80] M. A. Parker *et al.* (BEBC TST Neutrino Collaboration), *Nucl. Phys. B* **232**, 1 (1984).
- [81] D. Allasia *et al.* (Amsterdam-Bergen-Bologna-Padova-Pisa-Saclay-Torino Collaboration), *Nucl. Phys. B* **239**, 301 (1984).
- [82] P. N. Shotton, W. Venus, and H. Wachsmuth, CERN EP/NBU/85-2, European Organization for Nuclear Research, Geneva, 1985 (unpublished).
- [83] M. Aderholz *et al.* (BEBC WA21 and BEBC WA59 Collaborations), *Phys. Lett. B* **173**, 211 (1986).
- [84] J. V. Allaby *et al.* (CHARM Collaboration), *Phys. Lett. B* **179**, 301 (1986).
- [85] J. P. Berge *et al.*, *Z. Phys. C* **35**, 443 (1987).
- [86] J. V. Allaby *et al.* (CHARM Collaboration), *Z. Phys. C* **38**, 403 (1988).
- [87] D. Allasia *et al.* (Amsterdam-Bergen-Bologna-Padova-Pisa-Saclay-Torino Collaboration), *Nucl. Phys. B* **343**, 285 (1990).
- [88] A. Kayis-Topaksu *et al.* (CHORUS Collaboration), *Eur. Phys. J. C* **30**, 159 (2003).
- [89] A. E. Asratyan *et al.* (Moscow-Serpukhov Collaboration), *Yad. Fiz.* **28**, 424 (1978) [*Sov. J. Nucl. Phys.* **28**, 214 (1978)]; *Phys. Lett. B* **76**, 239 (1978).
- [90] D. S. Baranov *et al.*, *Yad. Fiz.* **29**, 1203 (1979) [*Sov. J. Nucl. Phys.* **29**, 620 (1979)]; *Phys. Lett. B* **81**, 255 (1979).
- [91] A. S. Vovenko *et al.*, *Yad. Fiz.* **30**, 1014 (1979) [*Sov. J. Nucl. Phys.* **30**, 527 (1979)].
- [92] V. V. Makeev *et al.*, *Pisma Zh. Eksp. Teor. Fiz.* **34**, 418 (1981) [*JETP Lett.* **34**, 397 (1981)].
- [93] S. V. Belikov *et al.*, *Yad. Fiz.* **35**, 59 (1982) [*Sov. J. Nucl. Phys.* **35**, 35 (1982)].
- [94] S. V. Belikov *et al.*, *Z. Phys. A* **320**, 625 (1985).
- [95] H. J. Grabosch *et al.*, *Yad. Fiz.* **47**, 1630 (1988) [*Sov. J. Nucl. Phys.* **47**, 1032 (1988)].
- [96] J. Brunner *et al.* (SKAT Collaboration), *Z. Phys. C* **42**, 361 (1989).
- [97] J. Brunner *et al.* (SKAT Collaboration), *Z. Phys. C* **45**, 551 (1990).
- [98] V. V. Ammosov *et al.*, *Fiz. Elem. Chast. Atom. Yadra* **23**, 648 (1992) [*Sov. J. Part. Nucl.* **23**, 283 (1992)].
- [99] V. B. Anikeev *et al.*, *Z. Phys. C* **70**, 39 (1996).
- [100] F. James, “MINUIT, Reference Manual, Version 94.1,” CERN Program Library Long Writeup D506 (European Organization for Nuclear Research, Geneva, 1994).
- [101] The relative error exceeding $\sim 10\%$ indicates that the fit is unsuccessful. The D3 version (Table III) with the BNL-2002 provoked trial value of M_A^{RES} provides an example of such a situation despite small χ^2 .
- [102] Actually the fit comprehends the primary data for heavy targets while the nuclear effects are included into the calculated QES cross sections.
- [103] R. Gran (for the K2K Collaboration), *Nucl. Phys. B (Proc. Suppl.)* **139**, 54 (2005).
- [104] Y. Ashie *et al.* (Super-Kamiokande Collaboration), *Phys. Rev. D* **71**, 112005 (2005) [hep-ex/0501064].
- [105] K. Hagiwara *et al.* (Particle Data Group), *Phys. Rev. D* **66**, 010001 (2002).